ELSEVIER

Chemical Geology 213 (2004) 115–123

CHEMICAL GEOLOGY
INCLUDING
ISOTOPE GEOSCIENCE

www.elsevier.com/locate/chemgeo

# Melt speciation in the system $Na_2O$–$SiO_2$

Werner E. Halter[a,*], Bjørn O. Mysen[b]

[a]*Institute for Isotope Geochemistry and Natural Resources, Department of Earth Sciences ETH Zurich, ETH Zentrum NO 8092 Zurich, Switzerland*

[b]*Geophysical Laboratory, The Carnegie Institution of Washington, 5251 Broad Branch Road, NW, Washington, DC 20015, USA*

Received 3 December 2003; received in revised form 4 June 2004; accepted 31 August 2004

**Abstract**

The applicability of a speciation model to quantify the thermodynamic properties of silicate liquids was evaluated in the $Na_2O$–$SiO_2$ system. Based on spectroscopic data, four sodium-silicate species with various numbers of bridging oxygen atoms were considered. We used a thermodynamic model that assumed ideal mixing between the species and temperature-independent, additive heat capacities of the species. Enthalpies and entropies of the melt species were determined by fitting experimental data.

Enthalpies and entropies for each species were determined by fitting either speciation data from spectroscopic investigations or experimental data on mineral–melt equilibrium assemblages. Results were evaluated by comparing the calculated species abundances and mineral–melt equilibrium temperature with the experimental data. No temperature or compositional dependence of the quality of the fit was observed. An independent check of the applicability of the model is provided by the fact that enthalpies and entropies of the species could be determined by fitting phase equilibrium data and used to reproduce the speciation data. The excellent overlap of the experiments and the calculated values shows that in this system, the speciation approach accurately reproduces melt properties. This evaluation of a speciation model suggests that it has a significant potential to describe thermodynamic and physicochemical properties of silicate liquids. Moreover, for melt compositions in which the speciation cannot be determined, information from phase diagrams can be used to resolve the speciation of the melt and, potentially, speciation-dependent properties (e.g., the viscosity).


*Keywords:* Speciation; Thermodynamic; Silicate liquid; Modeling; Fitting

## 1. Introduction

Determination of mineral–melt phase equilibria and quantitative information on macroscopic properties of silicate melts require accurate knowledge of the thermodynamic properties of the melt phase. Experimental studies are powerful means to provide such information, but they can only be performed at specific pressures, temperatures and compositions. Conditions relevant to natural systems can often not be reproduced in the laboratory. For a comprehensive understanding of melt properties, existing experimen-

* Corresponding author. Fax: +41 1 632 18 27.
*E-mail address:* halter@erdw.ethz.ch (W.E. Halter).

0009-2541/$ - see front matter © 2004 Elsevier B.V. All rights reserved.
doi:10.1016/j.chemgeo.2004.08.036

tal data needs to be extrapolated. This additional step requires the use of thermodynamic models.

Several models have been developed to calculate thermodynamic properties of silicate melts in binary and multicomponent systems. In the material sciences, models such as THERMOCALC AB or FACTS have successfully describe phase equilibria in binary and some ternary systems (Pelton et al., 1997, 2000; Blander, 2000). In multicomponent systems, the MELTS (Ghiorso and Sack, 1995) and Thermocalc (Holland and Powell, 1998, 2001) models have provided highly valuable information on the behavior of basaltic and granitic systems, respectively. All these models have in common that they describe properties of silicate melts through the properties of a minimum number of components and a specific mixing model to quantify properties of intermediate compositions. These components are not, however, representative of the structural species that exist in the melts.

In the last two decades, the rapid development of analytical techniques such as Nuclear Magnetic Resonance (NMR) or Raman and infrared spectroscopy has allowed a significant progress in the understanding of silicate melt structures (McMillan et al., 1992; Stebbins et al., 1992, 1995; Mysen and Frantz, 1992, 1994; Mysen, 1995, 1997; Mysen, 1999; McMillan and Wolf, 1995; Stebbins, 1995; Richet and Bottinga, 1995; Maekawa and Yokokawa, 1997). With these techniques, it was established that melts are a combination of a relatively small number of species and that changes in physical and thermodynamic properties of melts mainly reflect a change in their relative abundance (Mysen, 2003).

The objective of this study is to evaluate the use and applicability of a speciation model to quantify thermodynamic properties of silicate liquids. In this model, liquids are described through the properties of the constituent species (rather than the components) and variations in melt properties are accounted for by variations in the relative abundance of these species. The idea of using a speciation model is that it makes use of the existing structural information on silicate melts and the combination with chemical data should yield a robust and broadly applicable model to derive melt properties. We selected the well-investigated $Na_2O$–$SiO_2$ system to conduct this test, as more data are available for this binary join than for other compositions.

## 2. Thermodynamic model

Spectroscopic studies have shown that silicate melts in the system $Na_2O$–$SiO_2$ are made of several sodium-silicate species, distinguished by their number of bridging oxygen atoms (see McMillan and Wolf, 1995 for a review). To minimize the difference in the thermodynamic properties of these species, we normalized the species to the same number of Si atoms, namely two. Thus, the species used in this study are $Si_2O_4$, $Na_2Si_2O_5$, $Na_4Si_2O_6$ and $Na_6Si_2O_7$, referred to as $Q^4$, $Q^3$, $Q^2$ and $Q^1$, respectively. For each $Q^n$, $n$ is the number of bridging oxygen atoms per silicon tetrahedra. The relative abundance of melt species is governed by the reactions

$$2Q^3 = Q^2 + Q^4 \quad (1)$$

and

$$2Q^2 = Q^1 + Q^3 \quad (2)$$

The compositions investigated range from $N3S2$ to pure silica, where $N$ is the number of moles of $Na_2O$ and $S$ the number of moles of $SiO_2$. More $Na_2O$-rich compositions were not retained, as they are not relevant to geological systems and no speciation data is available to check the validity of the approach at high Na contents. In addition, because of the large difference in the properties of pure $Na_2O$ and Si-bearing species, the ideal mixing assumption might not be valid.

The free energy $G$ of a species $i$ at a given temperature $T$ is described by

$$G_{iT} = H_{iT_r} + \int_{T_r}^{T} C_{p_i} \mathrm{d}T - T\left(S_{iT_r} + \int_{T_r}^{T} \frac{C_{p_i}}{T} \mathrm{d}T\right) \quad (3)$$

where $H_i$ is the enthalpy, $S_i$ the entropy and $C_{p_i}$ the heat capacity of the species $i$. $T_r$ is the reference temperature of 298 K.

In $Na_2O$–$SiO_2$ melts, several studies have shown that heat capacities can be accurately described through the relative contribution of the components, and that these heat capacities are independent of the temperature (Richet et al., 1984; Wu et al., 1993; Tangeman and Lange, 1998). In this study, we will use this information to calculate $C_p$ for the various species by adding the partial contributions of the

Table 1
Speciation data in the $SiO_2$–$Na_2O$ system

| Composition | Temperature (°C) | Species abundances | | |
|---|---|---|---|---|
| | | $Q^2$ | $Q^3$ | $Q^4$ |
| NS2 | 469 | 0.084 | 0.832 | 0.084 |
| | 505 | 0.121 | 0.758 | 0.121 |
| | 527 | 0.091 | 0.817 | 0.091 |
| | 571 | 0.098 | 0.803 | 0.098 |
| | 572 | 0.130 | 0.741 | 0.130 |
| | 620 | 0.086 | 0.829 | 0.086 |
| | 637 | 0.134 | 0.732 | 0.134 |
| | 669 | 0.107 | 0.785 | 0.107 |
| | 700 | 0.154 | 0.691 | 0.154 |
| | 718 | 0.113 | 0.774 | 0.113 |
| | 771 | 0.149 | 0.702 | 0.149 |
| | 773 | 0.119 | 0.762 | 0.119 |
| | 825 | 0.120 | 0.760 | 0.120 |
| | 833 | 0.159 | 0.683 | 0.159 |
| | 878 | 0.133 | 0.734 | 0.133 |
| | 899 | 0.153 | 0.693 | 0.153 |
| | 929 | 0.139 | 0.723 | 0.139 |
| | 961 | 0.147 | 0.705 | 0.147 |
| | 996 | 0.136 | 0.728 | 0.136 |
| | 1024 | 0.160 | 0.679 | 0.160 |
| | 1052 | 0.140 | 0.721 | 0.140 |
| | 1087 | 0.163 | 0.674 | 0.163 |
| | 1144 | 0.159 | 0.683 | 0.159 |
| | 1205 | 0.161 | 0.677 | 0.161 |
| | 1267 | 0.165 | 0.669 | 0.165 |
| | 1326 | 0.165 | 0.670 | 0.165 |
| *NS*3 | 516 | 0.047 | 0.572 | 0.380 |
| | 586 | 0.056 | 0.555 | 0.389 |
| | 643 | 0.053 | 0.561 | 0.386 |
| | 692 | 0.053 | 0.560 | 0.386 |
| | 746 | 0.058 | 0.552 | 0.391 |
| | 798 | 0.059 | 0.548 | 0.392 |
| | 866 | 0.066 | 0.535 | 0.399 |
| | 914 | 0.061 | 0.545 | 0.394 |
| | 961 | 0.068 | 0.532 | 0.401 |
| | 1021 | 0.072 | 0.524 | 0.405 |
| | 1074 | 0.070 | 0.528 | 0.403 |
| | 1118 | 0.078 | 0.511 | 0.411 |
| *NS*4 | 637 | 0.012 | 0.475 | 0.512 |
| | 700 | 0.013 | 0.475 | 0.513 |
| | 771 | 0.017 | 0.466 | 0.517 |
| | 833 | 0.013 | 0.473 | 0.513 |
| | 899 | 0.017 | 0.466 | 0.517 |
| | 961 | 0.018 | 0.464 | 0.518 |
| | 1024 | 0.018 | 0.465 | 0.518 |
| | 1087 | 0.019 | 0.462 | 0.519 |
| | 1144 | 0.018 | 0.464 | 0.518 |
| | 1205 | 0.017 | 0.466 | 0.517 |
| | 1267 | 0.020 | 0.459 | 0.520 |
| | 1326 | 0.021 | 0.458 | 0.521 |
| | 1386 | 0.021 | 0.459 | 0.521 |
| | 1386 | 0.021 | 0.457 | 0.521 |
| *NS*4 | 1457 | 0.019 | 0.462 | 0.519 |
| | 1523 | 0.025 | 0.451 | 0.525 |
| *NS*5 | 771 | 0.005 | 0.391 | 0.605 |
| | 899 | 0.006 | 0.389 | 0.606 |
| | 1024 | 0.006 | 0.388 | 0.606 |
| | 1144 | 0.008 | 0.383 | 0.608 |
| | 1267 | 0.007 | 0.386 | 0.607 |
| | 1386 | 0.007 | 0.386 | 0.607 |
| | 1457 | 0.008 | 0.384 | 0.608 |
| | 1523 | 0.009 | 0.382 | 0.609 |
| | 1587 | 0.007 | 0.386 | 0.607 |
| | 1651 | 0.011 | 0.379 | 0.611 |
| *NS*7 | 787 | 0.008 | 0.271 | 0.721 |
| | 920 | 0.007 | 0.272 | 0.720 |
| | 1052 | 0.005 | 0.277 | 0.718 |
| | 1165 | 0.007 | 0.273 | 0.720 |
| | 1214 | 0.005 | 0.278 | 0.718 |
| | 1279 | 0.005 | 0.277 | 0.718 |
| | 1338 | 0.005 | 0.277 | 0.718 |
| | 1401 | 0.007 | 0.274 | 0.720 |
| | 1463 | 0.006 | 0.274 | 0.719 |
| | 1535 | 0.009 | 0.270 | 0.722 |
| | 1608 | 0.008 | 0.271 | 0.721 |

components. Thus, to describe the free energy of the species, we need to fit only their respective enthalpies and the entropies at the reference temperature.

To determine properties of bulk liquids, we assume that species mix ideally, i.e., that the configurational entropy is given by the mixing of the Q-species and that there is no excess free energy of mixing between the species. The former assumption could be improved by using viscosity data to constrain the entropy of mixing in the calculation (Toplis, 2001). The latter assumption is justified by the fact that most energetic changes in this system occur when Si is added to pure $Na_2O$ melt (Navrotsky, 1995). The choice of using only $SiO_2$-bearing species drastically reduces the interaction energies between the species, i.e., any excess free energy of mixing. The same assumption of ideal mixing was successfully used by Gurman (1990) in a similar approach to investigate this $Na_2O$–$SiO_2$ system.

The assumption of ideal mixing between the species precludes an accurate description of the liquid–liquid immiscibility that occurs at high $SiO_2$ contents (e.g., Vedishcheva et al., 1998; Hovis et al., 2004) and which affect properties of glasses at low

temperatures (Jarry and Richet, 2001) and the properties of the liquids (Hovis et al., 2004). Description of this miscibility gap requires the use of interaction parameters, presumably between $Q^3$ and $Q^4$ species. However, this miscibility gap closes at 1110 K, and this interaction does not appear to influence the high temperature modeling conducted in this study. Thus, the interaction parameter cannot be accurately determined with this approach and was neglected.

## 3. Existing data

### 3.1. Spectroscopic data

Mysen and Frantz (1992, 1993) used Raman spectroscopy to measure the relative abundance of species as a function of temperature and composition in silica-rich melts of the $Na_2O$–$SiO_2$ binary system. Quantification of the species abundance was obtained by calibrating Raman cross sections with NMR measurements on glasses of the same composition. These studies assumed that calibration factors were independent of the composition, and recent measurements revealed that this is not strictly correct. Thus, new calibration factors for several compositions along this binary were acquired and the Raman data was reinterpreted (Cody et al., 2001; Mysen et al., 2003; Mysen, unpublished data). For compositions *NS*5 and *NS*7, the calibration factors were obtained by interpolating existing data of the $Q^3$ abundance as a function of the composition. The speciation data used in this study are reported in Table 1 and plotted in Fig. 1.

Speciation data provide very strong constraints on the thermodynamic properties of melt species as the temperature and compositional dependence of the species abundance permits a direct quantification of the enthalpy and entropy of the species.

### 3.2. Phase equilibria

Equilibrium conditions between solids and melts are well known in the system under investigation and a summary of the available data is presented in Wu et al. (1993). In the present study, we used the 23 experimental points with bulk liquid compositions of between 41 and 96 mol% $SiO_2$ to fit the thermodynamic properties of the different species. These liquids

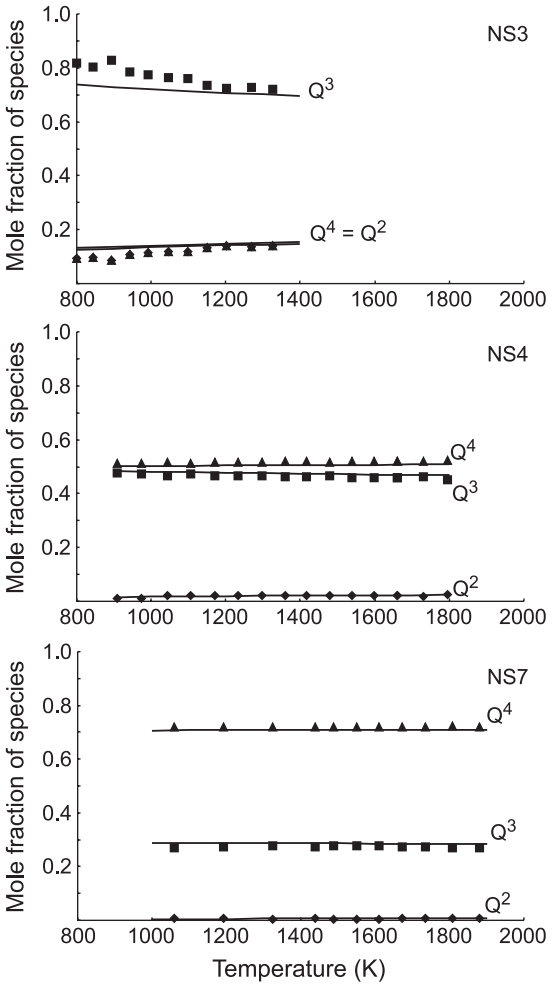


Fig. 1. Measured and calculated species abundances as a function of temperature for various compositions. Symbols are measured species abundances, reported in Table 1, and used to fit thermodynamic properties of melt species. Lines are the calculated species abundances using the thermodynamic properties obtained by fitting this data.

are in equilibrium with six solid phases (Fig. 2). Wu et al. (1993) also presented an internally consistent data set for the mineral properties. At the mineral–melt equilibrium conditions, these data constrain the properties of bulk silicate liquids. However, they provide no information on the relative abundance of the species.

### 3.3. Thermodynamic data

Heat capacities for the melt species were obtained by combining heat capacities of the components

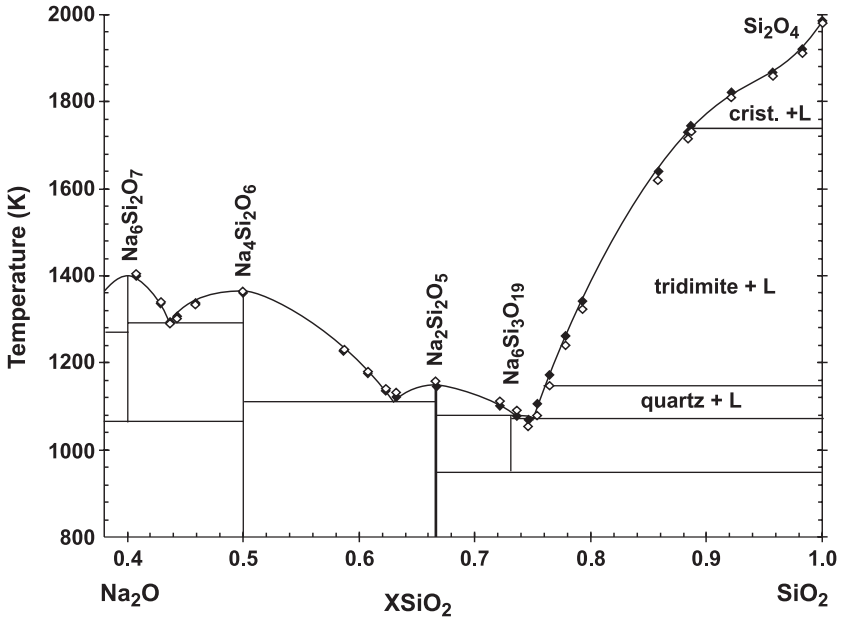


Fig. 2. Phase relationships in the system $Na_2O$–$SiO_2$. Solid symbols are the experimentally determined mineral–melt equilibrium conditions. These experiments were used to determine a second, independent set of thermodynamic properties for the melt species. These properties were used to reproduce mineral melt equilibrium conditions (open symbols).

determined by Richet et al. (1984). Thus, for $Q^4$ to $Q^1$, the values of $C_p$ are 162.74, 263.34, 363.94 and 464.54 J/mol·K, respectively.

In pure silica systems, thermodynamic properties of the liquid can be obtained through the properties of cristobalite and its enthalpy and entropy of fusion. In sodium-free liquids, $Si_2O_4$ is the only species present, and the properties of this species were quantified directly from the properties of the bulk liquids. Taking the data on cristobalite from Wu et al. (1993) and the enthalpy and entropy of fusion from Richet and Bottinga (1986), this yields an enthalpy and entropy for the $Q^4$ species of −1 844 109 J/mol and 34.86 J/mol·K, respectively (Table 2).

For the solids $Na_2Si_2O_5$ (*NS*2) and $Na_4Si_2O_6$ (*N*2*S*2), the enthalpy and entropy of fusion are also known (Richet and Bottinga, 1986). In contrast to the pure silica system, liquids of the same compositions consist of several species as reactions (1) and (2) imply that at least three Q-species coexist. Spectroscopic data suggest, however, that the $Q^3$ species forms most of the *NS*2 melt (e.g., Mysen and Frantz, 1993). Thus, the properties of $Q^3$ are closely approximated by the properties of the solid phase plus the enthalpy and entropy of fusion (Table 2). Assuming that $Q^2$ is the dominant species at the composition *N*2*S*2 (as suggested from the NMR data of its glass, see, for example, Maekawa et al., 1991),

Table 2
Standard state thermodynamic properties of silicate melt species at 25 °C and 1 bar

| Species | Estimated[a] | From speciation data[b] | From mineral–melt equilibria[c] |
|---|---|---|---|
| *Enthalpies (J/mol)* | | | |
| $Si_2O_4$ | −1 844 109 | −1 844 109 | −1 844 109 |
| $Na_2Si_2O_5$ | −2 458 850 | −2 460 907 | −2 464 252 |
| $Na_4Si_2O_6$ | −3 073 733 | −3 071 044 | −3 075 727 |
| $Na_6Si_2O_7$ | | | −3 658 200 |
| *Entropies (J/mol·K)* | | | |
| $Si_2O_4$ | 34.86 | 34.86 | 34.86 |
| $Na_2Si_2O_5$ | 136.56 | 124.77 | 124.31 |
| $Na_4Si_2O_6$ | 194.28 | 194.12 | 193.11 |
| $Na_6Si_2O_7$ | | | 234.26 |

[a] Estimates using properties of solids at the melting temperature from Wu et al. (1993), enthalpies and entropies of fusions form Richet and Bottinga (1986) and heat capacities from Richet et al. (1984).
[b] Fitted using measured species abundances from Table 1.
[c] Fitted using mineral–melt equilibria summarized by Wu et al. (1993).

the properties of the $Q^2$ species can also be approximated by the properties of solid $Na_4Si_2O_6$ and the enthalpy and entropy of fusion. Bulk liquid properties were used to constrain the fitting of the spectroscopic data at the temperature of fusion.

## 4. Quantification of thermodynamic properties

Thermodynamic properties of silicate melt species can be obtained through two approaches, making use of (1) the speciation data or (2) constraints from phase equilibria and mineral properties. We used both approaches independently to permit a comparison of the results and, thus, an evaluation of the thermodynamic model. In both cases, the data on $Si_2O_4$ was taken as a starting constraint.

### 4.1. Thermodynamic properties from speciation data

At equilibrium, the change in the free energy for reactions (1) and (2) is zero, and, thus

$$\Delta G_T = \Delta G_T^{\circ} + RT\ln K = 0 \tag{4}$$

where $\Delta G_T^{\circ}$ is the change in the standard state free energy at the temperature $T$, $R$ is the gas constant and $K$ is the equilibrium constant of each reaction. For reaction (1), $\Delta G_T^{\circ}$ is given by

$$\Delta G_T^{\circ} = G_T^{\circ Q^2} + G_T^{\circ Q^4} - 2G_T^{\circ Q^3} \tag{5}$$

and the equilibrium constant $K$ is given by

$$K = \frac{a_{Q^2} a_{Q^4}}{a_{Q^3}^2} \tag{6}$$

where $a_Q^i$ is the activity of the species $i$ in the melt. Assuming ideal mixing (i.e., no excess free energy of mixing), the equilibrium constant becomes

$$K = \frac{x_{Q^2} x_{Q^4}}{x_{Q^3}^2} \tag{7}$$

where $x_Q^i$ is the mole fraction of the species $i$. Similar equations can be written for reaction (2). By using the spectroscopically determined abundances of $x_Q^i$ at various temperatures and compositions, the standard state properties of the species can be fitted at $T$r by substituting Eqs. (5) and (7) into Eq. (4) and using constraints from the free energy of fusion of the solids.

### 4.2. Thermodynamic properties from phase equilibria

Equilibrium between minerals and melts requires that the chemical potential μ of a component be the same in both phases. For instance, for melts in equilibrium with cristobalite

$$\mu_{Si_2O_4}^{\text{cristobalite}} = \mu_{Si_2O_4}^{\text{melt}} \tag{8}$$

Similar equations can be written for the other species and the corresponding mineral phases. In a melt where ideal mixing is assumed and using pure mineral phases, Eq. (8) implies that

$$G_i^{\text{solid}} = H_{iT_r}^L + \int_{T_r}^{T} C_{P_i}^L \mathrm{d}T - T\left(S_{iT_r}^L + \int_{T_r}^{T} \frac{C_{P_i}^L}{T}\mathrm{d}T\right) + RT\ln x_i \tag{9}$$

where the exponent $L$ refers to the properties in the liquid. Thus, fitting the thermodynamic properties requires that $x_i$ be defined at each experimental point. This can be achieved by solving a non-linear set of four equations, including a mass balance equation, the sum of the mole fractions and the two equilibrium conditions between the melt species given by Eqs. (1) and (2). As the latter two equations are, in turn, dependent on the thermodynamic properties of the species, these equations need to be solved simultaneously with Eq. (9). For the solution to be unique, data also need to be constrained by the abundance of the melt species at the mineral–melt equilibrium conditions.

## 5. Results

For each species in the melt, two sets of parameters are obtained using the two approaches mentioned above (Table 2). Values of these parameters for $Q^1$ could not be obtained from speciation data, as these do not extend to sufficiently high $Na_2O$ contents for the $Q^1$ species to have significant concentrations.

The values of the thermodynamic parameters obtained with the speciation data and the phase equilibrium data are within a few percent of each

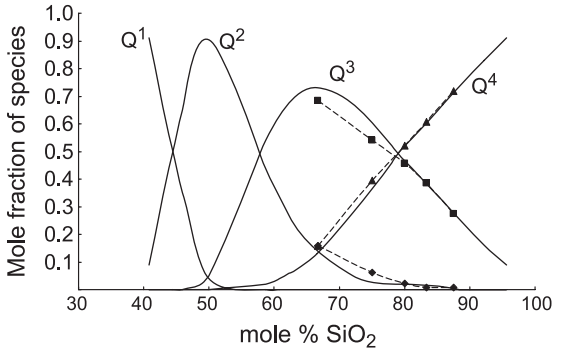


Fig. 3. Change in the abundance of melt species as a function of the composition at the mineral–melt equilibrium temperatures. Open symbols represent measures values and solid lines are calculated using thermodynamic properties for melt species obtained by fitting phase equilibria.

other and close to the values estimated using the solid phases and the entropies and enthalpies of melting (Table 2). This is remarkable as the databases used to fit the parameters provide completely different information. To evaluate the accuracy with which melt species can reproduce properties of the melt at the various experimental conditions, we used the two sets of fitted thermodynamic properties to reproduce the experimental data from which they were obtained.

The thermodynamic properties of the species obtained by fitting the measured species abundances (column 2 in Table 2) are compared to the actual values (from Table 1) in Fig. 1. The plots in Fig. 1 show that the experimental data are accurately reproduced at all temperatures and compositions. Thus, over the conditions under investigation, the properties of the melt species and the assumptions made in the thermodynamic model permit a reliable description of the changes in the species abundance of the melt.

In Fig. 2, we evaluate the accuracy with which this speciation model reproduces the experimentally determined phase diagram over the compositional range investigated. In this case, we used the thermodynamic properties for the species obtained by fitting the mineral–melt equilibrium data (column 3 in Table 2). Calculations reproduce the experimental conditions within a few degrees over the entire compositional range. As for the speciation data, no systematic temperature or compositional effect on the quality of the fit is apparent. The largest deviations are observed where the liquid is in equilibrium with quartz as significant amounts of Na are present in the melt, yet, the solid only constraints the properties of $Si_2O_4$.

## 6. Discussion

The results in Figs. 1 and 2 suggest that in the $Na_2O$–$SiO_2$ system, the speciation approach accurately reproduces the thermodynamic properties of the bulk liquid and, thus, the phase equilibria and the

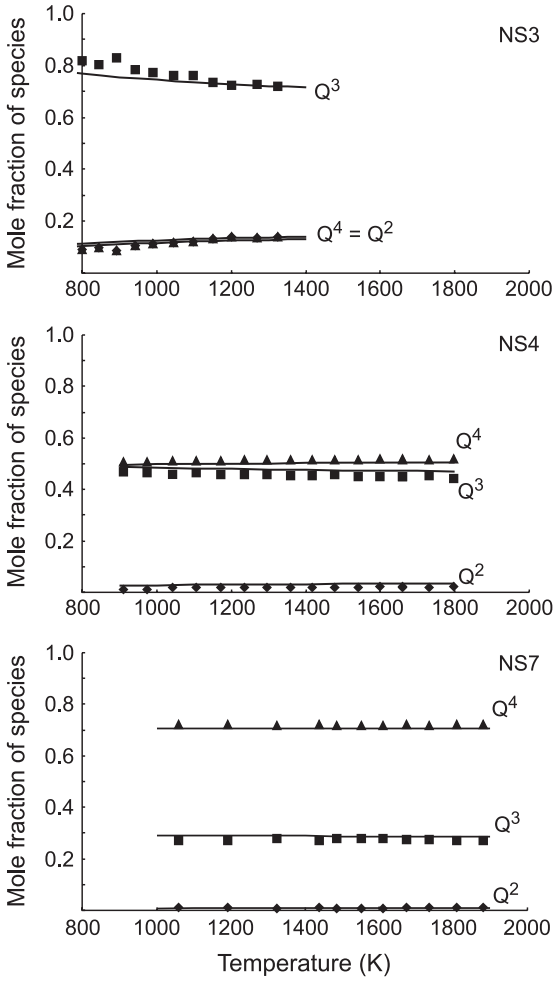


Fig. 4. Comparison between the measured speciation and the species abundances calculated using thermodynamic properties obtained from phase equilibria. The close fit of the data by the model shows that information from phase diagrams can be used to accurately model the speciation of the melt.

speciation data over the range of temperature and composition over which the parameters were fitted. Information on melt speciation is available only for a limited number of binary and ternary systems as the Raman spectra of chemically complex liquids cannot be resolved. Thus, the model is only useful if the thermodynamic properties for melt species, determined by fitting mineral–melt equilibrium data, can be used to quantify the speciation.

We used the thermodynamic properties of the species, determined from phase equilibrium data, to calculate variations in the speciation as a function of the composition at the temperatures at which solids and liquid co-exist (Fig. 3). Results of these calculations were compared to the spectroscopically determined speciation data. Except for small discrepancies, the calculated speciation can closely reproduce the abundance of the species. In particular, the variation in the speciation with composition is clearly reproduced. It is interesting to note that the $Q^3$ species appears to be less stable than $Q^2$, which is consistent with the fact that $Q^2$ should have lower configurational entropy because of its symmetry.

The measured and calculated changes in the speciation as a function of temperature at various compositions are compared in Fig. 4. As in Fig. 3, the thermodynamic data used for the calculation are those determined by fitting the phase diagram. From these plots, it appears that the temperature dependence of species abundance is remarkably well reproduced with this model. This is true at any composition and for all the species considered in this study. The applicability of this model to other systems, and particularly to multicomponent systems remains to be evaluated.

The results in Figs. 3 and 4 show that thermodynamic properties derived from phase equilibria accurately reproduce the compositional and temperature variation of the speciation. This result has several implications. First, it strongly supports the validity of the thermodynamic model. In particular, it shows that ideal mixing between melt species is a valid assumption in the temperature and compositional range investigated. Thus, the benefit of adding structural information to the thermodynamic model is that it largely overcomes the necessity of using interaction terms. It cannot entirely substitute their use, as interaction terms are necessary to describe liquid–liquid immiscibility (Hovis et al., 2004). Second, it shows that we can extract accurate information on the melt speciation from mineral–melt equilibrium assemblages, i.e., the thermodynamic properties determined from phase diagrams can be used to gain insight into the speciation of the melt. This implies that even in the absence of detailed spectroscopic data, e.g., in multicomponent systems, the speciation of the melt and speciation dependent properties can be constrained.

## Acknowledgments

This research was supported by the Swiss National Science Foundation Grant PP002-68687 to WH. We would like to thank Mike Toplis and two anonymous reviewers for their constructive comments on the manuscript. **[RR]**

## References

Blander, M., 2000. Fundamental theories and concepts for predicting thermodynamic properties of high temperature ionic and metallic liquid solutions and vapor molecules. Metall. Mater. Trans., B, Process Metall. Mater. Process. Sci. 31 (4), 579–586.

Cody, G.D., Mysen, B., Saghi-Szabo, G., Tossell, J.A., 2001. Silicate–phosphate interactions in silicate glasses and melts: I. A multinuclear (Al-27,Si-29,P-31) MAS NMR and ab initio chemical shielding (P-31) study of phosphorous speciation in silicate glasses. Geochim. Cosmochim. Acta 65 (14), 2395–2411.

Ghiorso, M.S., Sack, R.O., 1995. Chemical mass-transfer in magmatic processes: 4. A revised and internally consistent thermodynamic model for the interpolation and extrapolation of liquid–solid equilibria in magmatic systems at elevated-temperatures and pressures. Contrib. Mineral. Petrol. 119 (2–3), 197–212.

Gurman, S.J., 1990. Bond ordering in silicate-glasses—a critique and a re-solution. J. Non-Cryst. Solids 125 (1–2), 151–160.

Holland, T.J.B., Powell, R., 1998. An internally consistent thermodynamic data set for phases of petrological interest. J. Metamorph. Geol. 16 (3), 309–343.

Holland, T., Powell, R., 2001. Calculation of phase relations involving haplogranitic melts using an internally consistent thermodynamic dataset. J. Petrol. 42 (4), 673–683.

Hovis, G.L., Toplis, M.J., richet, P., 2004. Thermodynamic mixing properties of sodium silicte liquids and imlications for liquid–liquid immiscibility. Chem. Geol. 213, 173–186.

Jarry, P., Richet, P., 2001. Unmixing in sodium-silicate melts: influence on viscosity and heat capacity. J. Non-Cryst. Solids 293, 232–237.

Maekawa, H., Yokokawa, T., 1997. Effects of temperature on silicate melt structure: a high temperature Si-29 NMR study of $Na_2Si_2O_5$. Geochim. Cosmochim. Acta 61 (13), 2569–2575.

Maekawa, H., Maekawa, T., Kawamura, K., Yokokawa, T., 1991. The structural groups of alkali silicate-glasses determined from Si-29 Mas-Nmr. J. Non-Cryst. Solids 127 (1), 53–64.

McMillan, P.F., Wolf, G.H., 1995. Vibrational spectroscopy of silicate liquids. In: Stebbins, J.F., McMillan, P.F., Dingwell, D.B. (Eds.), Structure, Dynamics and Properties of Silicate Melts, Reviews in Mineralogy. Mineralogical Society of America, pp. 247–315.

McMillan, P.F., Wolf, G.H., Poe, B.T., 1992. Vibrational spectroscopy of silicate liquids and glasses. Chem. Geol. 96 (3–4), 351–366.

Mysen, B., 1995. Experimental, in-situ, high-temperature studies of properties and structure of silicate melts relevant to magmatic processes. Eur. J. Mineral. 7 (4), 745–766.

Mysen, B., 1997. Aluminosilicate melts: structure, composition and temperature. Contrib. Mineral. Petrol. 127 (1–2), 104–118.

Mysen, B., 2003. Physics and chemistry of silicate glasses and melts. Eur. J. Mineral. 15 (5), 781–802.

Mysen, B.O., 1999. Structure and properties of magmatic liquids: from haplobasalt to haploandesite. Geochim. Cosmochim. Acta 63 (1), 95–112.

Mysen, B., 2003. Physics and chemistry of silicate glasses and melts. Eur. J. Mineral. (In press).

Mysen, B.O., Frantz, J.D., 1992. Raman-spectroscopy of silicate melts at magmatic temperatures—$Na_2O$–$SiO_2$, $K_2O$–$SiO_2$ and $Li_2O$–$SiO_2$ binary compositions in the temperature-range 25–1475 °C. Chem. Geol. 96 (3–4), 321–332.

Mysen, B.O., Frantz, J.D., 1993. Structure and properties of alkali silicate melts at magmatic temperatures. Eur. J. Mineral. 5 (3), 393–407.

Mysen, B.O., Frantz, J.D., 1994. Structure of haplobasaltic liquids at magmatic temperatures—in-situ, high-temperature study of melts on the join $Na_2Si_2O_5$–$Na_2(NaAl)_2O_5$. Geochim. Cosmochim. Acta 58 (7), 1711–1733.

Mysen, B.O., Lucier, A., Cody, G.D., 2003. The structural behaviour of $Al^{3+}$ in peralkaline melts and glasses in the system $Na_2O$–$Al_2O_3$–$SiO_2$. Am. Mineral. 88 (11–12), 1668–1678.

Navrotsky, A., 1995. Energetics of silicate melts. In: Stebbins, J.F., McMillan, P., Dingwell, D.B. (Eds.), Structure, Dynamics and Properties of Silicate Melts, Reviews in Mineralogy. Mineralogical Society of America, pp. 121–143.

Pelton, A.D., Blander, M., Clavaguera Mora, M.T., Hoch, M., Hoglund, L., Lukas, H.L., Spencer, P., Sundman, B., 1997. Thermodynamic modeling of solutions and alloys—Schloss Ringberg, March 10–16, 1996—Group 1: liquids. Calphad-Comput. Coupling Phase Diagr. Thermochem. 21 (2), 155–170.

Pelton, A.D., Degterov, S.A., Eriksson, G., Robelin, C., Dessureault, Y., 2000. The modified quasichemical model I—binary solutions. Metall. Mater. Trans., B, Process Metall. Mater. Process. Sci. 31 (4), 651–659.

Richet, P., Bottinga, Y., 1986. Thermochemical properties of silicate-glasses and liquids—a review. Rev. Geophys. 24 (1), 1–25.

Richet, P., Bottinga, Y., 1995. Rheology and configurational entropy of silicate melts. In: Stebbins, J.F., McMillan, P.F., Dingwell, D.B. (Eds.), Structure, Dynamics and Properties of Silicate Melts, Reviews in Mineralogy. Mineralogical Society of America, pp. 67–93.

Richet, P., Bottinga, Y., Tequi, C., 1984. Heat-capacity of sodium-silicate liquids. J. Am. Ceram. Soc. 67 (1), C6–C8.

Stebbins, J.F., 1995. Dynamics and structure of silicate and oxide melts: nuclear magnetic resonance studies. Structure, Dynamics and Properties of Silicate Melts, Reviews in Mineralogy. Mineralogical Society of America, pp. 191–246.

Stebbins, J.F., Farnan, I., Xue, X.Y., 1992. The structure and dynamics of alkali silicate liquids—a view from NMR-spectroscopy. Chem. Geol. 96 (3–4), 371–385.

Stebbins, J.F., Sen, S., Farnan, I., 1995. Silicate species exchange, viscosity, and crystallization in a low-silica melt—in-situ high-temperature MAS NMR-spectroscopy. Am. Mineral. 80 (7–8), 861–864.

Tangeman, J.A., Lange, R.A., 1998. The effect of $Al^{3+}$, $Fe^{3+}$, and $Ti^{4+}$ on the configurational heat capacities of sodium silicate liquids. Phys. Chem. Miner. 26 (2), 83–99.

Toplis, M.J., 2001. Quantitative links between microscopic properties and viscosity of liquids in the system $SiO_2$–$Na_2O$. Chem. Geol. 174 (1–3), 321–331.

Vedishcheva, N.M., Shakhmatkin, B.A., Wright, A.C., 1998. A thermodynamic approach to the structural modeling of oxide melts and glasses: borate and silicate systems. Glass Phys. Chem. 24 (4), 308–311.

Wu, P., Eriksson, G., Pelton, A.D., 1993. Optimization of the thermodynamic properties and phase-diagrams of the $Na_2O$–$SiO_2$ and $K_2O$–$SiO_2$ systems. J. Am. Ceram. Soc. 76 (8), 2059–2064.